



Clinical and Prognostic Implications of Right Ventricular Uptake on Bone Scintigraphy in Transthyretin Amyloid Cardiomyopathy

Aldostefano Porcari¹, MD; Marianna Fontana¹, MD, PhD; Marco Canepa¹, MD, PhD; Elena Biagini¹, MD; Francesco Cappelli¹, MD, PhD; Christian Gagliardi¹, MD; Simone Longhi¹, MD; Linda Pagura¹, MD; Giacomo Tini¹, MD; Franca Dore¹, MD; Rachele Bonfiglioli¹, MD; Matteo Bauckneht¹, MD; Alberto Miceli, MD; Francesca Girardi, MD; Anna Lisa Martini¹, MD; Giulia Barbati, PhD; Egidio Natalino Costanzo, MD; Angelo Giuseppe Caponetti¹, MD; Andrea Paccagnella¹, MD; Maurizio Sguazzotti¹, MD; Giovanni La Malfa¹, MD; Mattia Zampieri¹, MD; Roberto Sciagrà¹, MD; Federico Perfetto¹, MD, PhD; Dorota Rowczenio, PhD; Janet Gilbertson, CSci; David F. Hutt¹, BAppSc; Philip N. Hawkins¹, MD, PhD; Claudio Rapezzi, MD; Marco Merlo¹, MD; Gianfranco Sinagra¹, MD*; Julian D. Gillmore, MD, PhD*

BACKGROUND: The extent of myocardial bone tracer uptake with technetium pyrophosphate, hydroxymethylene diphosphonate, and 3,3-diphosphono-1,2-propanodicarboxylate in transthyretin amyloid cardiomyopathy (ATTR-CM) might reflect cardiac amyloid burden and be associated with outcome.

METHODS: Consecutive patients with ATTR-CM who underwent diagnostic bone tracer scintigraphy with acquisition of whole-body planar and cardiac single-photon emission computed tomography (SPECT) images from the National Amyloidosis Centre and 4 Italian centers were included. Cardiac uptake was defined according to the Perugini classification: 0=absent cardiac uptake; 1=mild uptake less than bone; 2=moderate uptake equal to bone; and 3=high uptake greater than bone. Extent of right ventricular (RV) uptake was defined as focal (basal segment of the RV free wall only) or diffuse (extending beyond basal segment) on the basis of SPECT imaging. The primary outcome was all-cause mortality.

RESULTS: Among 1422 patients with ATTR-CM, RV uptake accompanying left ventricular uptake was identified by SPECT imaging in 100% of cases at diagnosis. Median follow-up in the whole cohort was 34 months (interquartile range, 21 to 50 months), and 494 patients died. By Kaplan-Meier analysis, diffuse RV uptake on SPECT imaging ($n=936$) was associated with higher all-cause mortality compared with focal ($n=486$) RV uptake (77.9% versus 22.1%; $P<0.001$), whereas Perugini grade was not associated with survival ($P=0.27$ in grade 2 versus grade 3). On multivariable analysis, after adjustment for age at diagnosis (hazard ratio [HR], 1.03 [95% CI, 1.02–1.04]; $P<0.001$), presence of the p.(V142I) *TTR* variant (HR, 1.42 [95% CI, 1.20–1.81]; $P=0.004$), National Amyloidosis Centre stage (each category, $P<0.001$), stroke volume index (HR, 0.99 [95% CI, 0.97–0.99]; $P=0.043$), E/e' (HR, 1.02 [95% CI, 1.007–1.03]; $P=0.004$), right atrial area index (HR, 1.05 [95% CI, 1.02–1.08]; $P=0.001$), and left ventricular global longitudinal strain (HR, 1.06 [95% CI, 1.03–1.09]; $P<0.001$), diffuse RV uptake on SPECT imaging (HR, 1.60 [95% CI, 1.26–2.04]; $P<0.001$) remained an independent predictor of all-cause mortality. The prognostic value of diffuse RV uptake was maintained across each National Amyloidosis Centre stage and in both wild-type and hereditary ATTR-CM ($P<0.001$ and $P=0.02$, respectively).

Correspondence to: Julian D. Gillmore, MD, PhD, National Amyloidosis Centre, Division of Medicine, University College London, Rowland Hill St, London NW1 2PF, UK. Email j.gillmore@ucl.ac.uk

*G. Sinagra and J.D. Gillmore contributed equally.

Supplemental Material is available at <https://www.ahajournals.org/doi/suppl/10.1161/CIRCULATIONAHA.123.066524>.

Continuing medical education (CME) credit is available for this article. Go to <http://cme.ahajournals.org> to take the quiz.

For Sources of Funding and Disclosures, see page 1166.

© 2024 The Authors. *Circulation* is published on behalf of the American Heart Association, Inc., by Wolters Kluwer Health, Inc. This is an open access article under the terms of the [Creative Commons Attribution Non-Commercial-NoDerivs](https://creativecommons.org/licenses/by-nc-nd/4.0/) License, which permits use, distribution, and reproduction in any medium, provided that the original work is properly cited, the use is noncommercial, and no modifications or adaptations are made.

Circulation is available at www.ahajournals.org/journal/circ

CONCLUSIONS: Diffuse RV uptake of bone tracer on SPECT imaging is associated with poor outcomes in patients with ATTR-CM and is an independent prognostic marker at diagnosis.

Key Words: amyloidosis ■ prognosis ■ tomography, emission-computed, single-photon ■ transthyretin

Editorial, see p 1169

Clinical Perspective

What Is New?

- Amyloid deposition in transthyretin amyloid cardiomyopathy (ATTR-CM) is widespread, with 100% of patients demonstrating biventricular uptake of bone tracers on single-photon emission tomography (SPECT) imaging, which cannot be reliably determined on planar imaging.
- Patients with ATTR-CM and diffuse, as opposed to focal, right ventricular uptake on SPECT have more advanced cardiac disease, evidenced by laboratory and echocardiographic parameters consistent with a higher amyloid burden.
- The extent of right ventricular uptake of bone tracers on SPECT imaging is independently associated with survival across all forms of ATTR-CM regardless of genotype (ie, wild-type or variant ATTR) or National Amyloidosis Centre stage.

What Are the Clinical Implications?

- Diffuse right ventricular uptake on SPECT imaging has the ability to identify patients with ATTR-CM at higher risk of mortality and is a novel independent prognostic marker.
- Cardiac scintigraphy with bone tracers with acquisition of planar and SPECT images has an established diagnostic value in ATTR-CM, but its prognostic role has been controversial. The findings of this study demonstrate a novel prognostic role of cardiac scintigraphy and provide a further reason to perform SPECT along with planar imaging to assess the presence and extent of right ventricular uptake.

Transthyretin amyloid (ATTR) cardiomyopathy (ATTR-CM) is a prevalent and emerging cause of heart failure and can lead to death.^{1,2} Although histological evidence of amyloid deposition remains the gold standard diagnostic technique, the validation of cardiac scintigraphy with bone tracers coupled with biochemical assays for nonbiopsy confirmation of ATTR-CM has revolutionized the ability to diagnose this condition.^{3,4} In patients with an echocardiogram that suggests amyloid who do not have biochemical evidence of a monoclonal gammopathy, the presence of high-grade myocardial uptake (ie, Perugini grade 2 or 3) identifies ATTR-CM

Nonstandard Abbreviations and Acronyms

ATTR	transthyretin amyloid
ATTR-CM	transthyretin amyloid cardiomyopathy
ATTRv-CM	variant transthyretin amyloid cardiomyopathy
HR	hazard ratio
IQR	interquartile range
LV	left ventricular
NAC	National Amyloidosis Centre
NT-proBNP	N-terminal pro-B-type natriuretic peptide
RV	right ventricular
SPECT	single-photon emission computed tomography
TTR	transthyretin

with high accuracy.^{5–8} Tracer retention in the heart is thought to be most prominent in the thickened left ventricle (LV), as suggested by recent reports.^{9–11} Recently, the use of single-photon emission computed tomography (SPECT) imaging^{8,12} has enabled a better understanding of bone tracer localization, including visualization of right ventricular (RV) uptake.

Despite the excellent diagnostic performance of bone scintigraphy, the prognostic impact of the Perugini grade has been evaluated in a few studies with conflicting results.^{13–18} We undertook a multicenter study in which we characterized the extent of RV uptake accompanying LV uptake on SPECT imaging among patients with ATTR-CM at diagnosis to establish whether it was associated with clinical outcomes.

METHODS

This was a multicenter, retrospective study performed at the UK National Amyloidosis Centre (NAC; London, UK) and in 4 Italian referral centers for cardiac amyloidosis (Trieste [Cattinara Hospital], Genoa [San Martino Hospital], Bologna [Sant'Orsola Hospital], and Florence [Careggi Hospital]). The NAC acted as coordinating center for the study. Local institutional review board approval for the study was obtained in each of the participating centers. The study was conducted according to the Declaration of Helsinki, and informed consent was obtained under the institutional review board policies of the relevant

hospital administrations. The data underlying this article cannot be shared publicly because of the privacy of individuals who participated in the study. The data will be shared on reasonable request to the corresponding author.

Study Population

Consecutive patients with ATTR-CM who underwent bone tracer scintigraphy with acquisition of both planar and SPECT images between January 1, 2015, and June 30, 2020, at participating centers were included in the study population. The diagnosis of ATTR-CM was established on the basis of heart failure symptoms together with a characteristic echocardiogram for amyloidosis or cardiac magnetic resonance imaging assessment, along with one of the following: (1) direct endomyocardial biopsy proof of ATTR amyloid, (2) presence of ATTR amyloid in an extracardiac biopsy along with diffuse cardiac uptake on nuclear scintigraphy, or (3) Perugini grade 2 or 3 myocardial uptake on cardiac scintigraphy in the absence of biochemical evidence of a monoclonal gammopathy. The date of bone tracer scintigraphy was defined as the date of diagnosis. Patients with light-chain amyloidosis were excluded. All patients underwent sequencing of the transthyretin (*TTR*) gene.¹⁹ The NAC ATTR staging system (from stage I–III) was defined on the basis of NT-proBNP (N-terminal pro-B-type natriuretic peptide; 3000 ng/L) and estimated glomerular filtration rate ($45 \text{ mL}\cdot\text{min}^{-1}\cdot 1.73 \text{ m}^{-2}$), as previously published.¹⁹

Echocardiography

Echocardiographic images stored on the electronic databases of the participating hospitals were systematically centrally reviewed in all study patients (Supplemental Material). All echocardiographic parameters were measured according to standard international definitions.²⁰ The presence and severity of valve disease were defined according to current recommendations.²¹

Nuclear Medicine

Characteristics of nuclear cameras, protocols for scan acquisition, and timing of image acquisition after bisphosphonate administration adopted in each participating center are shown in Table S1. Cardiac scintigraphy was performed with different bone tracers according to center local practice, namely ^{99m}Tc-pyrophosphate, ^{99m}Tc-3,3-diphosphono-1,2-propanodicarboxylic acid, and ^{99m}Tc-hydroxymethylene diphosphonate. Cardiac scintigraphy scans with both planar and SPECT images were centrally analyzed for this study (D.H., F.D., F.G., R.B., A.M., and M.B.). A modified Perugini grade was obtained on planar images as previously described.²² Planar biventricular uptake was defined in presence of LV and RV uptake on planar images. In detail, RV uptake on planar images using the frontal plane was defined in presence of (1) bone tracer retention near or below the right lower sternal border, resembling the position of the RV in the chest, or (2) radiotracer accumulation extending beyond the LV with visualization of the RV contour. LV and RV uptake was evaluated from SPECT images and defined as present or absent. The extent of LV and RV uptake was classified as focal, defined as uptake limited to the basal segment of the ventricular free wall, and diffuse, defined as uptake extending beyond the basal segment of the ventricular

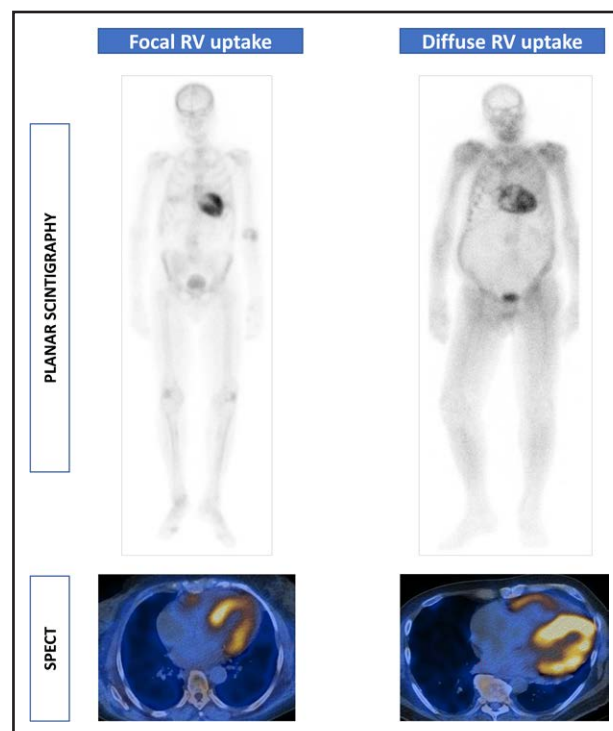


Figure 1. Extent of RV retention leading to biventricular uptake of bone tracers on planar and SPECT scintigraphy in transthyretin amyloid cardiomyopathy.

Top, Whole-body scans, anterior view. **Bottom**, Cross-sectional views of cardiac single-photon emission computed tomography (SPECT) in the same patients. **Left**, Focal right ventricular (RV) uptake: absent planar RV uptake but focal uptake in the basal RV free wall on SPECT. **Right**, Diffuse RV uptake: planar left ventricular and RV uptake with diffuse uptake in the RV free wall on SPECT.

free wall (Figure 1). Image analysis was independently performed by 6 operators (3 with >10 years of expertise in nuclear medicine) blinded to all patient data.

Study Outcomes

The primary outcome of the study was all-cause mortality. The censor date was June 30, 2022. All mortality data were obtained from the central National Health Service patient care records for the UK cohort and from the dedicated electronic databases of participating centers or telephone contact with general practitioners, patients, or relatives for the Italian cohort. Follow-up was restricted to ≤ 60 months, after which patients were censored because the majority of events had occurred during the first 60 months, and a low number of patients were at risk after 60 months. To control for the impact of disease-modifying therapy on survival, patients were censored on the start date of beginning *TTR* stabilizers, gene silencers, or enrollment in a therapeutic clinical trial.

TTR Gene Sequencing

All patients with ATTR-CM underwent sequencing of the *TTR* gene. DNA was extracted from whole blood and amplified by polymerase chain reaction assay, and the whole coding region of the *TTR* gene was sequenced as previously described.²³

Statistical Analysis

Descriptive statistics between the study groups were performed. Continuous variables were expressed as median with interquartile range (IQR; 25th, 75th percentile) because data were not normally distributed according to the results of the Kolmogorov-Smirnov test. Categorical variables were expressed as absolute numbers and percentages. Differences between groups were evaluated with the Mann-Whitney test for continuous variables, whereas the χ^2 or Fisher exact test was used for dichotomous variables. The Cronbach α was calculated to assess interoperator variability regarding the evaluation of biventricular uptake among operators. Survival was evaluated with Cox proportional hazard regression analysis, providing estimated hazard ratios (HRs) with 95% CIs, and Kaplan-Meier curves were compared with the log-rank test. The proportional hazards assumption was checked and confirmed. The primary survival analysis was performed with a multivariable Cox proportional hazards regression adjusting for covariates that were selected a priori on the basis of their clinical relevance according to previously established independent prognostic value in ATTR-CM, coupled with absence of collinearity among the remaining variables associated with survival at univariable analysis.^{19,21} Possible collinearity among candidate predictors was assessed with variance inflation factors with a threshold of 5. The final list of candidate predictors included age, p.(V142I) *TTR* variant, diabetes, NAC ATTR stage, stroke volume index, E/e', right atrial area index, LV global longitudinal strain, Perugini grade, and diffuse RV uptake. We defined a value of $P < 0.05$ as statistically significant. All statistical analyses were performed with IBM SPSS Statistics 24.0 package (New York, NY) statistical software version 20 and R (R Foundation for Statistical Computing, Vienna, Austria; <https://r-project.org/>).

RESULTS

Study Population

The study population consisted of 1422 patients, of whom 1298 (91%) were diagnosed at the UK NAC, and 8 were diagnosed in Bologna. All 1306 patients from these 2 centers received 3,3-diphosphono-1,2-propanodicarboxylate and were imaged 3 hours after injection with the same imaging acquisition protocol. Eighty-nine patients (from Genoa and Florence) received hydroxymethylene diphosphonate with image acquisition after 150 minutes, and 27 patients (from Trieste) received technetium pyrophosphate with image acquisition at 60 minutes. Baseline characteristics of the whole cohort are summarized in Table 1. In brief, 87.5% were male, median age at diagnosis was 78 years (IQR, 72–83 years), 24.3% had variant ATTR-CM, and 48.8% had NAC stage II or greater. On echocardiography, median interventricular septum thickness was 17 mm (IQR, 15–18 mm), and median LVEF, tricuspid annular plane systolic excursion, and LV global longitudinal strain were 50% (IQR, 43%–56%), 16 mm (IQR, 12–20), and -10.7 (IQR, -8.4 to -13.4), respectively.

Biventricular uptake on planar imaging was identified in 1217 patients (85%), and its presence corre-

lated with Perugini grade: 19.4% in Perugini grade 1, 87.7% in Perugini grade 2, and 93.5% in Perugini grade 3 ($P < 0.001$). However, on SPECT imaging, all patients had LV and RV free wall uptake and were reclassified as having biventricular uptake (Figure 1). Compared with 486 patients (34.2%) with focal RV uptake, those with diffuse RV uptake on SPECT imaging ($n=936$, 65.8%) were more frequently in NAC stage II or greater (54.3% versus 38%; $P < 0.001$) and had higher NT-proBNP (3020 ng/dL versus 1960 ng/dL; $P < 0.001$), higher interventricular septum thickness (17 mm versus 16 mm; $P < 0.001$), lower LVEF (50% versus 53%; $P < 0.001$), lower tricuspid annular plane systolic excursion (15 mm versus 17 mm; $P < 0.001$), and lower LV global longitudinal strain (-10.4% versus -11.8% ; $P < 0.001$). There was no association between extent of RV uptake and age (79 years versus 78 years; $P=0.06$), sex (88.4% versus 85.8% male; $P=0.16$), or genotype (24.4% versus 24.3%, variant ATTR-VM [ATTRv-CM]; $P=0.97$). In addition, there was no association between extent of RV uptake and the specific bone tracer or imaging center. Of note, on SPECT imaging, diffuse LV uptake was found in 97.7% of cases ($n=1390$), and all patients with diffuse RV uptake were also found to have diffuse LV uptake (Supplemental Material).

Prognostic Impact of Extent of RV Uptake

During a median follow-up of 34 months (IQR, 21–50 months), 494 patients died, 385 (77.9%) with diffuse RV uptake and 109 (22.1%) with focal RV uptake. By Kaplan-Meier analysis, diffuse RV uptake was associated with a greater risk of all-cause mortality ($P < 0.001$; Figure 2), with a net separation of the survival curves at 10 months from ATTR-CM diagnosis. However, Perugini grade was not associated with mortality (Perugini grade 2 versus grade 3; $P=0.27$).

Variables associated with all-cause mortality on univariable analysis are shown on the left side of Table 2. Multivariable analyses included a total of 1201 patients (84.5% of the study population). After adjustment for age at diagnosis (HR, 1.03; $P < 0.001$), presence of the p.(V142I) *TTR* variant (HR, 1.42; $P=0.004$), NAC ATTR stage ($P < 0.001$), stroke volume index (HR, 0.98; $P=0.043$), E/e' (HR, 1.02; $P=0.004$), right atrial area index (HR, 1.05; $P=0.001$), and LV global longitudinal strain (HR, 1.06; $P < 0.001$), diffuse RV uptake on SPECT imaging (HR, 1.60; $P < 0.001$) remained an independent predictor of all-cause mortality (Table 2, right side). For all included variables in this analysis, the variable inflation factor was < 3.5 .

When stratified by genotype, diffuse RV uptake on SPECT was associated with higher risk of all-cause mortality compared with focal RV uptake in both wild-type ATTR-CM ($P < 0.001$) and ATTRv-CM ($P=0.02$; Supplemental Material), although the extent of RV uptake was

Table 1. Baseline Clinical, Electrocardiographic, and Echocardiographic Characteristics of the Study Population

	Available data	Study population (n=1422)	Focal RV uptake (n=486)	Diffuse RV uptake (n=936)	P value
Age, y	1422	78 (72–83)	79 (71–83)	78 (73–83)	0.95
Male, n (%)	1422	1244 (87.5)	417 (85.8)	827 (88.4)	0.17
ATTRv-CM, n (%)	1422	346 (24.3)	118 (24.3)	228 (22.4)	0.97
p.(V142I) TTR, n (%)	1422	191 (13.4)	63 (13.0)	128 (13.7)	0.70
Race and ethnicity, n (%)	1422				0.60
White		1188 (83.5)	397 (81.7)	791 (84.5)	
Afro-Caribbean		218 (15.3)	83 (17.1)	135 (14.4)	
Asian		11 (0.8)	4 (0.8)	7 (0.7)	
Other		5 (0.4)	2 (0.4)	3 (0.3)	
Hypertension, n (%)	1309	496 (37.9)	196 (45.5)	300 (34.2)	<0.001
Diabetes, n (%)	1422	204 (14.3)	69 (14.2)	135 (14.4)	0.90
Stroke/TIA, n (%)	1309	140 (10.7)	47 (10.9)	93 (10.6)	0.86
Atrial fibrillation, n (%)	1422	736 (51.8)	250 (51.4)	486 (51.9)	0.86
PPM, n (%)	1422	145 (10.2)	49 (10.1)	96 (10.3)	0.92
Laboratory values					
eGFR, mL·min ⁻¹ ·1.73 m ⁻²	1415	60 (48–74)	62 (50–75)	59 (47–74)	0.011
NT-proBNP, ng/dL	1373	2728 (1357–5060)	1960 (937–3954)	3022 (1689–5465)	<0.001
NAC ATTR stage, n (%)	1372				<0.001
I		704 (51.3)	289 (62.3)	415 (45.6)	
II		485 (35.4)	123 (26.4)	362 (39.9)	
III		183 (13.3)	52 (11.3)	131 (14.4)	
Echocardiography values					
IVS, mm	1422	17 (15–18)	16 (14–17)	17 (16–19)	<0.001
PW, mm	1422	16 (15–18)	15 (13–17)	17 (16–18)	<0.001
RWT	1394	0.74 (0.62–0.86)	0.68 (0.56–0.81)	0.78 (0.66–0.90)	<0.001
LVM index, g/m ²	992	169 (139–208)	159 (129–196)	174 (144–214)	<0.001
LVEF, %	1422	50 (43–56)	53 (45–60)	50 (42–55)	<0.001
LVEF <50%, n (%)	1422	641 (45.6)	187 (39.1)	454 (48.9)	<0.001
SV index, mL/m ²	1373	20.9 (16.4–25.9)	22.6 (17.2–28.5)	20.5 (16.1–25.8)	0.010
LV-GLS, %	1256	−10.7 (−13.4 to −8.4)	−11.9 (−15.0 to −9.4)	−10.4 (−12.8 to −8.2)	<0.001
LAA index, cm ² /m ²	1266	13.2 (11.3–15.4)	12.6 (10.8–15.3)	13.4 (11.6–15.4)	0.001
RAA index, cm ² /m ²	1266	12.2 (10.1–14.7)	11.8 (9.2–14.1)	12.6 (10.1–14.5)	0.019
E/e'	1362	15 (12–20)	14 (11–18)	15.5 (12–20)	<0.001
TAPSE, mm	1319	16 (12–19)	17 (13–20)	15 (12–19)	<0.001
S' RV	1088	10 (8–12)	11 (9–13)	10 (8–12)	<0.001
sPAP, mmHg	885	37 (26–46)	37 (25–47)	37 (27–45)	0.74
Cardiac scintigraphy, n (%)					
Perugini grade	1422				<0.001
1		62 (4.4)	60 (12.3)	2 (0.2)	
2		1133 (79.6)	381 (78.4)	752 (80.3)	
3		227 (16)	45 (9.3)	182 (19.4)	

ATTR indicates transthyretin amyloid; ATTRv-CM, variant transthyretin amyloid cardiomyopathy; eGFR, estimated glomerular filtration rate; IVS, interventricular septum; LAA, left atrial area; LV-GLS, left ventricular global longitudinal strain; LVEF, left ventricular ejection fraction; LVM, left ventricular mass; MR, mitral regurgitation; NAC, National Amyloidosis Centre; NT-proBNP, N-terminal pro-B-type natriuretic peptide; p.(V142I), valine-to-isoleucine substitution at position 142; PPM, permanent pacemaker; PW, posterior wall; RAA, right atrial area; RV, right ventricle; RWT, relative wall thickness; sPAP, systolic pulmonary arterial pressure; SV, stroke volume; TAPSE, tricuspid annular plane systolic excursion; TIA, transient ischemic attack; TTR, transthyretin; and TR, tricuspid regurgitation.

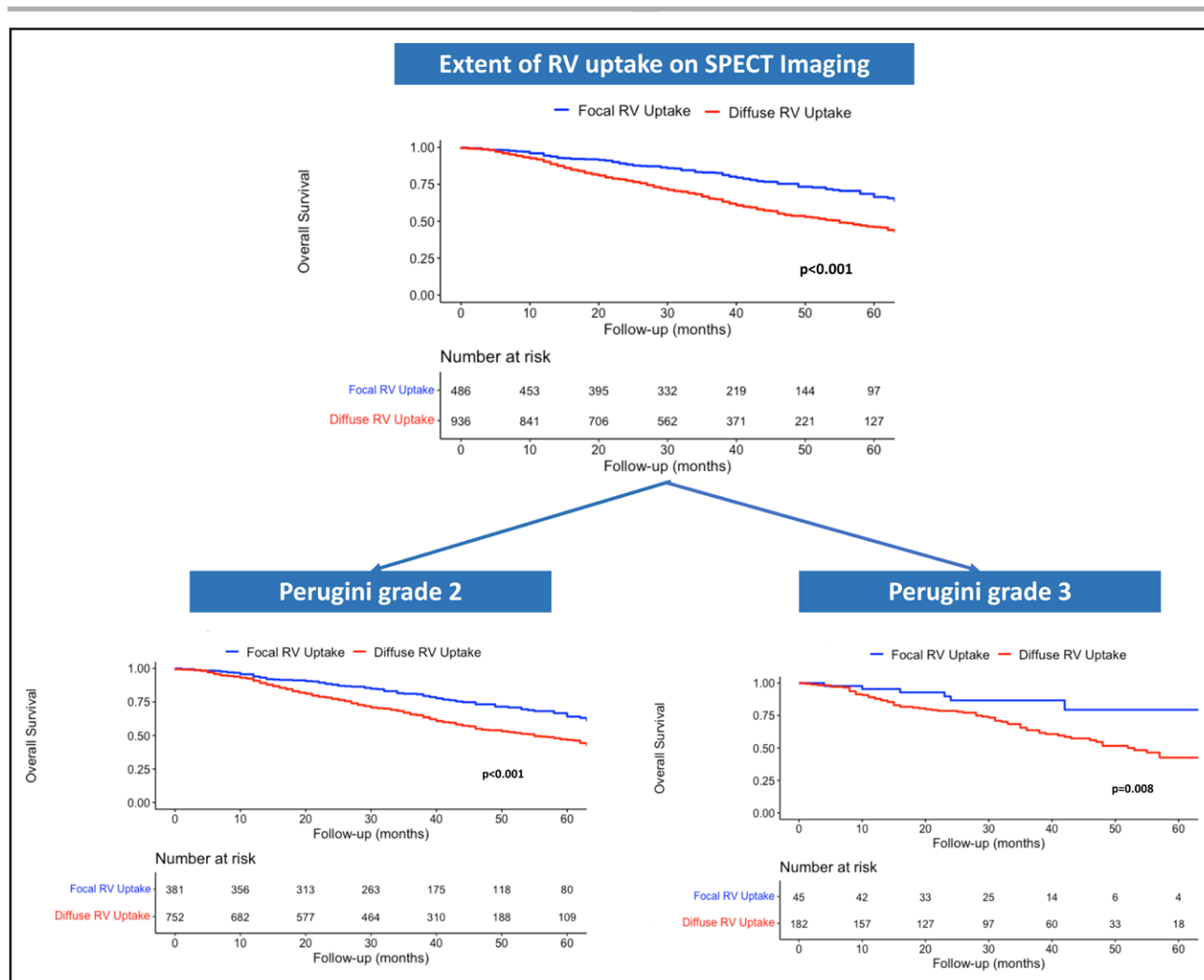


Figure 2. Kaplan-Meier survival curves stratified by (top) presence of focal vs diffuse RV uptake on SPECT imaging, (bottom left) in Perugini grade 2, and (bottom right) in Perugini grade 3.

RV indicates right ventricular; and SPECT, single-photon emission computed tomography.

not predictive of survival among those with ATTRv-CM associated with the p.(V142I) *TTR* variant ($P=0.11$; Figure 3). The prognostic value of the extent of RV uptake was confirmed in each individual NAC stage (Figure 3).

These findings were further confirmed in a sensitivity analysis in the UK cohort (Supplemental Material).

Intercenter Variability

There was good reliability between the centers in the assessment of Perugini classification ($P=0.88$), poor reliability for the assessment of RV uptake on planar imaging ($P=0.61$), and excellent reliability for the assessment of RV uptake on SPECT imaging ($P=0.99$; Table S2).

DISCUSSION

This study of >1400 consecutive patients with ATTR-CM who underwent bone tracer scintigraphy with both planar

and SPECT imaging is the first to evaluate the prevalence and to demonstrate the prognostic significance of the extent of RV uptake. The main findings of the study are: (1) biventricular uptake is present in 100% patients in this study with ATTR-CM on SPECT imaging, which is not reliably determined on planar imaging; (2) interoperator variability of SPECT images among expert readers was low; (3) among patients with ATTR-CM, those with diffuse RV uptake had more severe disease and higher all-cause mortality compared with patients who have focal RV uptake; and (4) from multivariable analysis, diffuse RV uptake on SPECT imaging was independently associated with worse overall survival and emerged as a novel prognostic marker in ATTR-CM. These data have potential implications for clinical practice, possibly providing information for patient-tailored follow-up and decision-making (Figure 4).

In the present analysis, we report that the prevalence of RV free wall uptake leading to biventricular uptake on

Table 2. Univariable and Multivariable Cox Regression Model for All-Cause Mortality

Variables	Missing data	Univariable model		Multivariable model*		
		HR (95% CI)	P value	Variables	HR (95% CI)	P value
Age	0	1.04 (1.02–1.05)	<0.001	Age	1.03 (1.02–1.04)	0.001
Male sex	0	1.06 (0.80–1.40)	0.66			
ATTRv-CM	0	1.12 (0.91–1.37)	0.27			
p.(V142I) TTR	0	1.46 (1.16–1.84)	0.001	p.(V142I) TTR	1.42 (1.20–1.81)	0.004
Diabetes	0	1.32 (1.05–1.66)	0.019	Diabetes	1.17 (0.92–1.50)	0.20
Hypertension	113	0.98 (0.81–1.18)	0.86			
Atrial fibrillation	0	1.16 (0.98–1.39)	0.09			
Stroke/TIA	113	0.93 (0.69–1.25)	0.63			
Pacemaker	0	1.01 (0.83–1.45)	0.51			
eGFR	7	0.97 (0.97–0.98)	<0.001			
NT-proBNP per each 400 ng/L	49	1.03 (1.03–1.04)	<0.001			
NAC ATTR Stage	50	Reference	<0.001	NAC ATTR stage	Reference	<0.001
II		2.56 (2.09–3.14)	<0.001	II	1.71 (1.35–2.16)	<0.001
III		3.34 (2.69–4.43)	<0.001	III	2.10 (1.58–2.80)	<0.001
IVS	0	1.11 (1.07–1.15)	<0.001			
RWT	28	3.91 (2.45–6.24)	<0.001			
LVM index	430	0.99 (0.99–1.01)	0.14			
LVEF, per 1%	0	0.96 (0.96–0.98)	<0.001			
LVEF <50%	0	1.95 (1.63–2.34)	<0.001			
SV index	49	0.96 (0.95–0.97)	<0.001	SV index	0.99 (0.97–0.99)	0.043
E/e'	60	1.02 (1.01–1.03)	<0.001	E/e'	1.02 (1.007–1.03)	0.004
LAA index	156	1.08 (1.05–1.10)	<0.001			
RAA index	156	1.08 (1.06–1.11)	<0.001	RAA index	1.05 (1.02–1.08)	0.001
TAPSE	103	0.94 (0.92–0.95)	<0.001			
LV-GLS	166	1.13 (1.10–1.16)	<0.001	LV-GLS	1.06 (1.03–1.09)	<0.001
Perugini grade	0	Reference	0.009	Perugini grade	Reference	0.57
2		2.70 (1.40–5.623)	0.003	2	1.31 (0.57–3.02)	0.52
3		2.95 (1.48–5.89)	0.002	3	1.15 (0.48–2.78)	0.75
Diffuse RV uptake	0	2.03 (1.64–2.51)	<0.001	Diffuse RV uptake	1.60 (1.26–2.04)	<0.001

ATTR indicates transthyretin amyloidosis; ATTRv-CM, variant transthyretin amyloid cardiomyopathy; eGFR, estimated glomerular filtration rate; HR, hazard ratio; IVS, interventricular septum; LAA, left atrial area; LV-GLS, left ventricular global longitudinal strain; LVEF, left ventricular ejection fraction; LVM, left ventricular mass; MR, mitral regurgitation; NAC, National Amyloidosis Centre; NT-proBNP, N-terminal pro-B-type natriuretic peptide; p.(V142I), valine-to-isoleucine substitution at position 142; PPM, permanent pacemaker; PW, posterior wall; RAA, right atrial area; RV, right ventricular; RWT, relative wall thickness; sPAP, systolic pulmonary arterial pressure; SV, stroke volume; TAPSE, tricuspid annular plane systolic excursion; TIA, transient ischemic attack; TTR, transthyretin; and TR, tricuspid regurgitation.

*A total of 1201 patients (84.5% of the study population) were included in the multivariable model.

bone tracer scintigraphy is 100% by SPECT imaging in this cohort, and we highlight the poor performance of planar imaging for evaluating RV uptake. These findings are not unexpected because of the diffuse nature of cardiac amyloid deposition^{24,25} and the greater accuracy of SPECT compared with planar imaging.^{8,12} SPECT imaging is recommended as part of routine acquisition protocols for diagnosis of ATTR-CM by international nuclear medicine societies to localize bone tracer uptake in the myocardium and to discriminate false-positive results attributable to blood pool artifact.²⁶ Our results provide another reason to perform SPECT after planar imaging,

which is to assess the presence and extent of RV uptake. Although each bone tracer has a specific protocol of image acquisition, findings from this study demonstrate that SPECT imaging is likely robust in assessing RV uptake independently of the specific bone tracer used to image amyloid in the heart. In our cohort, despite a similar age at diagnosis, patients with ATTR-CM with diffuse RV uptake had clinical, echocardiographic, and laboratory parameters consistent with a higher amyloid burden compared with those with focal RV uptake, including higher NAC stage, increased interventricular septum thickness, relative wall thickness and cardiac mass, and

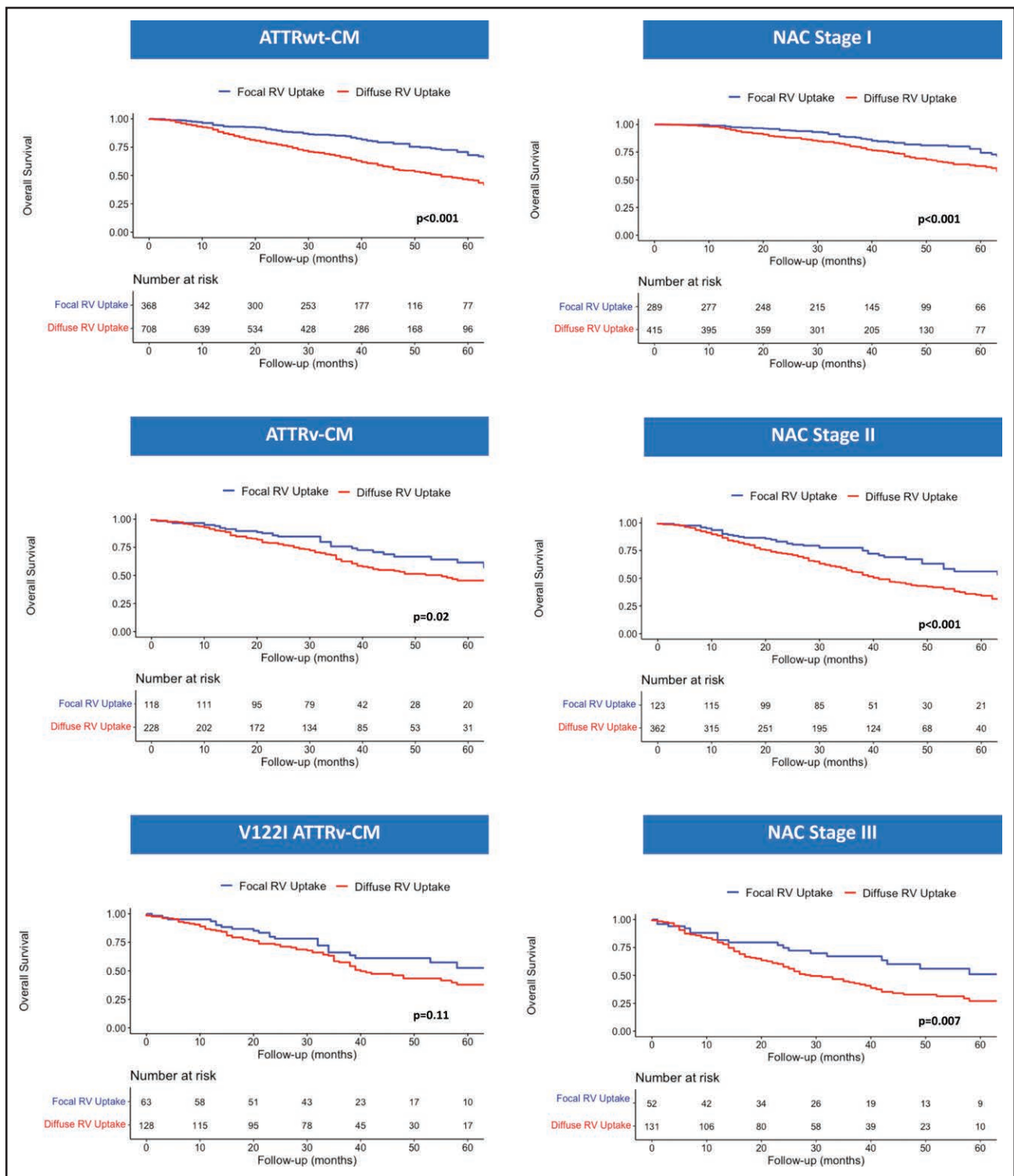


Figure 3. Kaplan-Meier survival curves stratified according to (left) genotype (ATTRwt vs ATTRv-CM) and (right) NAC stage.

The table shows the absolute numbers of patients at risk at different follow-up times. ATTRv-CM indicates variant transthyretin amyloid cardiomyopathy; ATTRwt-CM, wild-type transthyretin amyloid cardiomyopathy; NAC, National Amyloidosis Centre; RV, right ventricular; and V122I ATTRv-CM, variant transthyretin amyloid cardiomyopathy associated with the valine-to-isoleucine substitution.

lower indexes of LV and RV systolic function. Therefore, we hypothesize that the incremental prognostic value of diffuse RV uptake on SPECT might simply reflect a greater amyloid burden.

The key finding of this study is that diffuse RV uptake of bone tracer at SPECT imaging is associated with worse outcomes in ATTR-CM. Although myocardial uptake at planar imaging (measured as Perugini visual score, ratio

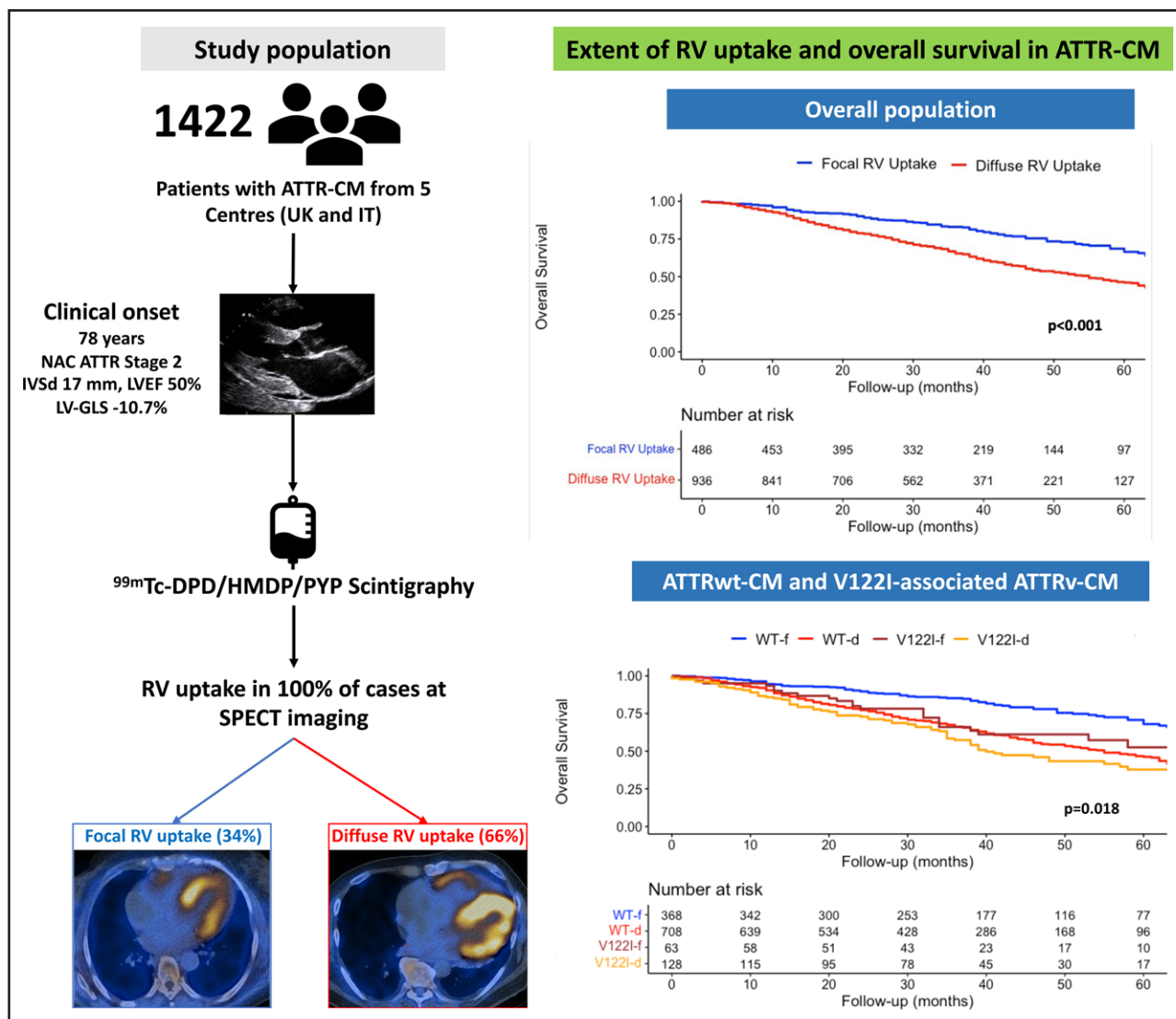


Figure 4. Proposal of a flowchart for prognostic stratification of patients with ATTR-CM according to the extent of right ventricular uptake on SPECT imaging.

ATTR-CM indicates transthyretin amyloid cardiomyopathy; IT, Italy; LV, left ventricular; NAC, National Amyloidosis Centre; SPECT, single-photon emission computed tomography; ^{99m}Tc-DPD, ^{99m}Tc-3,3-diphosphono-1,2-propanodicarboxylic acid; ^{99m}Tc-HMDP, ^{99m}Tc-hydroxymethylene diphosphonate; ^{99m}Tc-PYP, ^{99m}Tc-pyrophosphate; V122I, valine-to-isoleucine substitution; and WT, wild-type.

of heart to contralateral, or ratio of heart to whole body) has established and unequivocal diagnostic value,²⁷ its prognostic role remains controversial.^{13–18} Different protocols for image acquisition and characteristics of specific bone tracers²⁸ may have influenced results from previous studies.^{15,16,18} In the present cohort, patients with ATTR-CM with diffuse RV uptake at SPECT imaging had a higher risk of all-cause mortality independent of other known clinical and laboratory prognostic features. Consistent with the fact that the presence and extent of cardiac involvement determine prognosis in amyloidosis generally,^{4,29} more diffuse cardiac involvement on imaging was associated with more severe heart failure and poorer outcomes. Indexes of RV function such as tricuspid annular plane systolic excursion and longitudinal strain have been shown to portend a

worse prognosis in cardiac amyloidosis,^{30,31} thus offering the rationale to hypothesize that other RV parameters such as extent of bone tracer retention in the RV free wall might play a role in outcome prediction. We provide new evidence that SPECT imaging has the ability to identify patients carrying an incremental risk not detected by Perugini grading. In line with previous studies, Perugini grade was not associated with all-cause mortality in our analysis. The addition of extent of RV uptake along with the Perugini grade allowed reclassification of the risk of death. Among patients with Perugini grades 2 and 3, focal RV uptake on SPECT was associated with a more favorable outcome compared with diffuse RV uptake (Figure 2). In addition, diffuse RV uptake maintained its prognostic value across each NAC stage (Figure 3), supporting the hypothesis that this parameter

might provide incremental value for risk stratification in patients with ATTR-CM on top of well-known clinical and laboratory parameters.³²

The extent of RV uptake was not associated with poorer survival in hereditary ATTR-CM associated with the p.(V142I) *TTR* variant; this may simply be a reflection of sample size or may indicate that other factors might drive patient outcomes in this specific population. It is interesting that in the study cohort, the presence of diffuse RV uptake in wild-type ATTR-CM identified a group of patients with a natural history approaching that of V122I-associated ATTRv-CM as a whole. Over recent years, it has become apparent that V122I-associated ATTRv-CM represents a particularly severe form of cardiac ATTR amyloidosis with poorer outcomes compared with other genotypic variants, including wild-type ATTR-CM.^{19,33–35}

The present data need to be interpreted within the limitations of the study. This retrospective study was conducted in referral centers for the diagnosis and management of ATTR-CM. Cardiac scintigraphy was performed with different cameras and bone tracers (all validated for diagnostic purposes) according to center local protocols. However, the evaluation of scintigraphy images was performed by experts in nuclear medicine and cardiac amyloidosis, the presence and extent of RV uptake was assessed by SPECT images in all cases, and interoperator variability for evaluation of scintigraphy images was low. Quantification of bone tracer uptake in the heart was not performed in this analysis and is a promising approach to be investigated in future dedicated studies. Cardiac magnetic resonance imaging data and RV global longitudinal strain data were not available for this analysis. Last, the results presented are from specialized amyloidosis referral centers; further work is required to establish whether our findings are generalizable to the full spectrum of patients with ATTR-CM, many of whom are diagnosed outside of specialist reference centers. Validation in large prospective future studies is warranted.

Conclusions

Amyloid deposition in ATTR-CM is likely widespread in both ventricles because 100% of the patients in the present study demonstrated RV uptake on SPECT imaging. Diffuse RV uptake was found in 66% of cases and was an independent predictor of mortality risk. These observations suggest that the extent of RV uptake on SPECT imaging might serve as a novel marker for prognostic stratification in ATTR-CM.

ARTICLE INFORMATION

Received July 28, 2023; accepted January 16, 2024.

Affiliations

National Amyloidosis Centre, Division of Medicine, University College London, UK (A.P., M.F., D.R., J.G., D.F.H., P.N.H., J.D.G.). Centre for Diagnosis and Treatment of Cardiomyopathies, Cardiovascular Department, Azienda Sanitaria Uni-

versitaria Giuliano-Isontina and University of Trieste, Italy (A.P., L.P., M.M., G.S.). European Reference Network for Rare, Low Prevalence and Complex Diseases of the Heart-ERN GUARD-Heart (A.P., E.B., C.G., S.L., L.P., A.G.C., M.S., M.M., G.S.). Cardiovascular Unit, IRCCS Ospedale Policlinico San Martino, Genova, Italy (M.C., G.L.M.). Department of Internal Medicine, University of Genova, Italy (M.C.). Cardiology Unit, IRCCS Azienda Ospedaliero-Universitaria di Bologna, Italy (E.B., C.G., S.L.). Tuscan Regional Amyloidosis Centre, Careggi University Hospital, Florence, Italy (F.C., F.P.). Cardiomyopathy Unit, Careggi University Hospital, University of Florence, Italy (F.C., M.Z.). Department of Clinical and Molecular Medicine, Sapienza University of Rome, Azienda Ospedaliera Universitaria Sant'Andrea, Italy (G.T.). Department of Nuclear Medicine, Azienda Sanitaria Universitaria Giuliano-Isontina and University of Trieste, Italy (F.D., F.G.). Department of Nuclear Medicine, IRCCS, University Sant'Orsola Hospital, University of Bologna, Italy (R.B., A.P.). Nuclear Medicine, IRCCS Ospedale Policlinico San Martino, Genova, Italy (M.B.). Nuclear Medicine, Department of Health Sciences (DISSAL), University of Genova, Italy (M.B.). Nuclear Medicine Unit, Azienda Ospedaliera S.S. Antonio e Biagio e Cesare Arrigo, Alessandria, Italy (A.M.). Nuclear Medicine Unit, Department of Experimental and Clinical Biomedical Sciences "Mario Serio," University of Florence, Careggi University Hospital, Italy (A.L.M., E.N.C., R.S.). Department of Medical Sciences, Biostatistics Unit, University of Trieste, Italy (G.B.). Department of Experimental, Diagnostic and Specialty Medicine, University of Bologna, Italy (A.G.C., M.S.). Cardiothoracic Department, University of Ferrara, Italy (C.R.). Maria Cecilia Hospital, GVM Care & Research, Cotignola, Ravenna, Italy (C.R.).

Acknowledgments

The authors thank all the nuclear medicine doctors, hematologists, neurologists, pathologists, and nephrologists of the participating centers for their essential contributions of multidisciplinary teams for the care of patients with amyloidosis. They thank Fondazione CRTrieste, Fondazione CariGO, Fincantieri, and all the health care professionals for the continuous support to the clinical management of patients affected by cardiomyopathies, followed in Heart Failure Outpatient Clinic of Trieste, and their families. Finally, special thanks go to the cardiac nurses of outpatient clinics involved in the study for their daily professional management of patients and their relatives. The authors particularly acknowledge the late Claudio Rapezzi, who was a giant of the amyloid field and made a significant contribution to this study.

Sources of Funding

For "Cardiology Unit, IRCCS Azienda Ospedaliero-Universitaria di Bologna, Bologna, Italy," the work reported in this publication was funded by the Italian Ministry of Health, RC-2022-2773270 project. No funding was received for other participating centers.

Disclosures

The authors report no conflicts in relation to the submitted work. They report the following conflicts outside the submitted work: Dr Rapezzi served on the Italian scientific advisory board of Pfizer and received unrestricted research grants and personal fees from Pfizer and personal fees from Alnylam Pharmaceuticals. Dr Biagini received advisory board fees from Sanofi, Genzyme, and Takeda. Dr Cappelli received advisory board fees from Pfizer and Akcea and research grants from Pfizer. Dr Sinagra received personal fees for occasional educational activities from Biotronik, Boston Scientific, AstraZeneca, and Novartis. Dr Canepa received speaker and advisor fees from Akcea Therapeutics, Menarini, Novartis, Pfizer, Sanofi e Sanofi Genzyme, and Vifor Pharma, as well as 2 investigator-initiated grants from Pfizer. Dr Fontana is supported by a British Heart Foundation intermediate clinical research fellowship (FS/18/21/33447). Dr Merlo received congress fees from Novartis and Vifor Pharma and research grant and congress fees from Pfizer. Dr Gillmore receives advisory board fees from Pfizer, Alnylam, ATTRalus, Intellia, AstraZeneca, and BridgeBio.

Supplemental Material

Expanded Methods
Figure S1
Tables S1–S6
References 36–41

REFERENCES

- Ioannou A, Patel RK, Razvi Y, Porcari A, Sinagra G, Venneri L, Bandera F, Masi A, Williams GE, O'Beara S, et al. Impact of earlier diagnosis in cardiac ATTR amyloidosis over the course of 20 years. *Circulation*. 2022;146:1657–1670. doi: 10.1161/CIRCULATIONAHA.122.060852

2. Porcari A, Rossi M, Cappelli F, Canepa M, Musumeci B, Cipriani A, Tini G, Barbati G, Varrà GG, Morelli C, et al. Incidence and risk factors for pacemaker implantation in light-chain and transthyretin cardiac amyloidosis. *Eur J Heart Fail*. 2022;24:1227–1236. doi: 10.1002/ehf.2533
3. Merlo M, Pagura L, Porcari A, Cameli M, Vergaro G, Musumeci B, Biagini E, Canepa M, Crotti L, Imazio M, et al. Unmasking the prevalence of amyloid cardiomyopathy in the real world: results from phase 2 of the AC-TIVE study, an Italian nationwide survey. *Eur J Heart Fail*. 2022;24:1377–1386. doi: 10.1002/ehf.2504
4. Porcari A, Merlo M, Rapezzi C, Sinagra G. Transthyretin amyloid cardiomyopathy: an uncharted territory awaiting discovery. *Eur J Intern Med*. 2020;82:7–15. doi: 10.1016/j.ejim.2020.09.025
5. Gillmore JD, Maurer MS, Falk RH, Merlini G, Damy T, Dispenzieri A, Wechalekar AD, Berk JL, Quarta CC, Grogan M, et al. Nonbiopsy diagnosis of cardiac transthyretin amyloidosis. *Circulation*. 2016;133:2404–2412. doi: 10.1161/CIRCULATIONAHA.116.021612
6. Garcia-Pavia P, Rapezzi C, Adler Y, Arad M, Basso C, Brucato A, Burazor I, Caforio ALP, Damy T, Eriksson U, et al. Diagnosis and treatment of cardiac amyloidosis: a position statement of the ESC Working Group on Myocardial and Pericardial Diseases. *Eur Heart J*. 2021;42:1554–1568. doi: 10.1093/eurheartj/ehab072
7. Perugini E, Guidalotti PL, Salvi F, Cooke RMT, Pettinato C, Riva L, Leone O, Farsad M, Ciliberti P, Bacchi-Reggiani L, et al. Noninvasive etiologic diagnosis of cardiac amyloidosis using 99m Tc-3,3-diphosphono-1,2-propanodicarboxylic acid scintigraphy. *J Am Coll Cardiol*. 2005;46:1076–1084. doi: 10.1016/j.jacc.2005.05.073
8. Dorbala S, Ando Y, Bokhari S, Dispenzieri A, Falk RH, Ferrari VA, Fontana M, Gheysens O, Gillmore JD, Glaudemans AWJM, et al. ASNC/AHA/ASE/EANM/HFSA/ISA/SCMR/SNMMI expert consensus recommendations for multimodality imaging in cardiac amyloidosis: part 2 of 2: diagnostic criteria and appropriate utilization. *J Card Fail*. 2019;25:854–865. doi: 10.1016/j.cardfail.2019.08.002
9. Grigoratos C, Aimo A, Rapezzi C, Genovesi D, Barison A, Aquaro GD, Vergaro G, Pucci A, Passino C, Marzullo P, et al. Diphosphonate single-photon emission computed tomography in cardiac transthyretin amyloidosis. *Int J Cardiol*. 2020;307:187–192. doi: 10.1016/j.ijcard.2020.02.030
10. Ross JC, Hutt DF, Burniston M, Page J, Steeden JA, Gillmore JD, Wechalekar AD, Hawkins PN, Fontana M. Quantitation of (99m)Tc-DPD uptake in patients with transthyretin-related cardiac amyloidosis. *Amyloid*. 2018;25:203–210. doi: 10.1080/13506129.2018.1520087
11. Scully PR, Morris E, Patel KP, Treibel TA, Burniston M, Klotz E, Newton JD, Sabharwal N, Kelion A, Manisty C, et al. DPD quantification in cardiac amyloidosis: a novel imaging biomarker. *JACC Cardiovasc Imaging*. 2020;13:1353–1363. doi: 10.1016/j.jcmg.2020.03.020
12. Dorbala S, Ando Y, Bokhari S, Dispenzieri A, Falk RH, Ferrari VA, Fontana M, Gheysens O, Gillmore JD, Glaudemans AWJM, et al. ASNC/AHA/ASE/EANM/HFSA/ISA/SCMR/SNMMI expert consensus recommendations for multimodality imaging in cardiac amyloidosis: part 1 of 2: evidence base and standardized methods of imaging. *J Card Fail*. 2019;25:e1–e39. doi: 10.1016/j.cardfail.2019.08.001
13. Sperry BW, Vranian MN, Tower-Rader A, Hachamovitch R, Hanna M, Brunken R, Phelan D, Cerqueira MD, Jaber WA. Regional variation in technetium pyrophosphate uptake in transthyretin cardiac amyloidosis and impact on mortality. *JACC Cardiovasc Imaging*. 2018;11:234–242. doi: 10.1016/j.jcmg.2017.06.020
14. Galat A, Rosso J, Guellich A, Van Der Gucht A, Rappeneau S, Bodez D, Guendouz S, Tissot C-M, Hittinger L, Dubois-Randé J-L, et al. Usefulness of 99m Tc-HMDP scintigraphy for the etiologic diagnosis and prognosis of cardiac amyloidosis. *Amyloid*. 2015;22:210–220. doi: 10.3109/13506129.2015.1072089
15. Hutt DF, Fontana M, Burniston M, Quigley A-M, Petrie A, Ross JC, Page J, Martinez-Naharro A, Wechalekar AD, Lachmann HJ, et al. Prognostic utility of the Perugini grading of 99mTc-DPD scintigraphy in transthyretin (ATTR) amyloidosis and its relationship with skeletal muscle and soft tissue amyloid. *Eur Heart J Cardiovasc Imaging*. 2017;18:1344–1350. doi: 10.1093/ehjci/jew325
16. Vranian MN, Sperry BW, Hanna M, Hachamovitch R, Ikram A, Brunken RC, Jaber WA. Technetium pyrophosphate uptake in transthyretin cardiac amyloidosis: associations with echocardiographic disease severity and outcomes. *J Nucl Cardiol*. 2018;25:1247–1256. doi: 10.1007/s12350-016-0768-9
17. Rapezzi C, Quarta CC, Guidalotti PL, Pettinato C, Fanti S, Leone O, Ferlini A, Longhi S, Lorenzini M, Reggiani LB, et al. Role of (99m)Tc-DPD scintigraphy in diagnosis and prognosis of hereditary transthyretin-related cardiac amyloidosis. *JACC Cardiovasc Imaging*. 2011;4:659–670. doi: 10.1016/j.jcmg.2011.03.016
18. Castano A, Haq M, Narotsky DL, Goldsmith J, Weinberg RL, Morgenstern R, Pozniakoff T, Ruberg FL, Miller EJ, Berk JL, et al. Multicenter study of planar technetium 99m pyrophosphate cardiac imaging: predicting survival for patients with ATTR cardiac amyloidosis. *JAMA Cardiol*. 2016;1:880–889. doi: 10.1001/jamacardio.2016.2839
19. Porcari A, Razi Y, Masi A, Patel R, Ioannou A, Rauf MU, Hutt DF, Rowczenio D, Gilbertson J, Martinez-Naharro A, et al. Prevalence, characteristics and outcomes of older patients with hereditary versus wild-type transthyretin amyloid cardiomyopathy. *Eur J Heart Fail*. 2023;25:515–524. doi: 10.1002/ehf.2776
20. Lang RM, Badano LP, Mor-Avi V, Afilalo J, Armstrong A, Ernande L, Flachskampf FA, Foster E, Goldstein SA, Kuznetsova T, et al. Recommendations for cardiac chamber quantification by echocardiography in adults: an update from the American Society of Echocardiography and the European Association of Cardiovascular Imaging. *Eur Heart J Cardiovasc Imaging*. 2015;16:233–270. doi: 10.1093/ehjci/jev014
21. Chacko L, Karia N, Venneri L, Bandera F, Passo BD, Buonamici L, Lazari J, Ioannou A, Porcari A, Patel R, et al. Progression of echocardiographic parameters and prognosis in transthyretin cardiac amyloidosis. *Eur J Heart Fail*. 2022;24:1700–1712. doi: 10.1002/ehf.2606
22. Hutt DF, Quigley A-M, Page J, Hall ML, Burniston M, Gopaul D, Lane T, Whelan CJ, Lachmann HJ, Gillmore JD, et al. Utility and limitations of 3,3-diphosphono-1,2-propanodicarboxylic acid scintigraphy in systemic amyloidosis. *Eur Heart J Cardiovasc Imaging*. 2014;15:1289–1298. doi: 10.1093/ehjci/jeu107
23. Rowczenio DM, Noor I, Gillmore JD, Lachmann HJ, Whelan C, Hawkins PN, Obici L, Westermarck P, Grateau G, Wechalekar AD. Online registry for mutations in hereditary amyloidosis including nomenclature recommendations. *Hum Mutat*. 2014;35:E2403–E2412. doi: 10.1002/humu.22619
24. Porcari A, Bussani R, Merlo M, Varrà GG, Pagura L, Rozze D, Sinagra G. Incidence and characterization of concealed cardiac amyloidosis among unselected elderly patients undergoing post-mortem examination. *Front Cardiovasc Med*. 2021;8:749523. doi: 10.3389/fcvm.2021.749523
25. Bandera F, Martone R, Chacko L, Ganesanathan S, Gilbertson JA, Ponticos M, Lane T, Martinez-Naharro A, Whelan C, Quarta C, et al. Clinical importance of left atrial infiltration in cardiac transthyretin amyloidosis. *JACC Cardiovasc Imaging*. 2022;15:17–29. doi: 10.1016/j.jcmg.2021.06.022
26. Dorbala S, Ando Y, Bokhari S, Dispenzieri A, Falk RH, Ferrari VA, Fontana M, Gheysens O, Gillmore JD, Glaudemans AWJM, et al. ASNC/AHA/ASE/EANM/HFSA/ISA/SCMR/SNMMI expert consensus recommendations for multimodality imaging in cardiac amyloidosis: part 1 of 2: evidence base and standardized methods of imaging. *Circ Cardiovasc Imaging*. 2021;14:e000029. doi: 10.1161/HCI.0000000000000029
27. Rauf MU, Hawkins PN, Cappelli F, Perfetto F, Zampieri M, Argiro A, Petrie A, Law S, Porcari A, Razi Y, et al. Tc-99m labelled bone scintigraphy in suspected cardiac amyloidosis. *Eur Heart J*. 2023;44:2187–2198. doi: 10.1093/eurheartj/ehad139
28. Porcari A, Hutt DF, Grigore SF, Quigley A-M, Rowczenio D, Gilbertson J, Patel R, Razi Y, Ioannou A, Rauf MU, et al. Comparison of different technetium-99m-labelled bone tracers for imaging cardiac amyloidosis. *Eur J Prev Cardiol*. 2022;30:e4–e6. doi: 10.1093/eurjpc/zwac237
29. Damy T, Kristen AV, Suhr OB, Maurer MS, Planté-Bordeneuve V, Yu C-R, Ong M-L, Coelho T, Rapezzi C. Transthyretin cardiac amyloidosis in continental Western Europe: an insight through the Transthyretin Amyloidosis Outcomes Survey (THAOS). *Eur Heart J*. 2019;43:391–400. doi: 10.1093/eurheartj/ehz173
30. Knight DS, Zumbo G, Barcella W, Steeden JA, Muthurangu V, Martinez-Naharro A, Treibel TA, Abdel-Gadir A, Bulluck H, Kotecha T, et al. Cardiac structural and functional consequences of amyloid deposition by cardiac magnetic resonance and echocardiography and their prognostic roles. *JACC Cardiovasc Imaging*. 2019;12:823–833. doi: 10.1016/j.jcmg.2018.02.016
31. Cohen OC, Ismael A, Pawarova B, Manwani R, Ravichandran S, Law S, Foard D, Petrie A, Ward S, Douglas B, et al. Longitudinal strain is an independent predictor of survival and response to therapy in patients with systemic AL amyloidosis. *Eur Heart J*. 2022;43:333–341. doi: 10.1093/eurheartj/ehab507
32. Gillmore JD, Damy T, Fontana M, Hutchinson M, Lachmann HJ, Martinez-Naharro A, Quarta CC, Rezak T, Whelan CJ, Gonzalez-Lopez E, et al. A new staging system for cardiac transthyretin amyloidosis. *Eur Heart J*. 2018;39:2799–2806. doi: 10.1093/eurheartj/ehx589
33. Quarta CC, Buxbaum JN, Shah AM, Falk RH, Claggett B, Kitzman DW, Mosley TH, Butler KR, Boerwinkle E, Solomon SD. The amyloidogenic

V122I transthyretin variant in elderly Black Americans. *N Engl J Med*. 2015;372:21–29. doi: 10.1056/NEJMoa1404852

34. Porcari A, Fontana M, Gillmore JD. Transthyretin cardiac amyloidosis. *Cardiovasc Res*. 2023;118:3517–3535. doi: 10.1093/cvr/cvac119
35. Razvi Y, Ioannou A, Patel RK, Chacko L, Karia N, Riefolo M, Porcari A, Rauf MU, Starr N, Ganesanathan S, et al. Deep phenotyping of p.(V142I)-associated variant ATTR amyloid cardiomyopathy: distinct from wild-type ATTR amyloidosis [published online November 13, 2023]? *Eur J Heart Fail*. 2023; doi: 10.1002/ehjhf.3088. <https://onlinelibrary.wiley.com/doi/10.1002/ehjhf.3088>
36. Tendler A, Helmke S, Teruya S, Alvarez J, Maurer MS. The myocardial contraction fraction is superior to ejection fraction in predicting survival in patients with AL cardiac amyloidosis. *Amyloid*. 2015;22:61–66. doi: 10.3109/13506129.2014.994202
37. Nagueh SF, Smiseth OA, Appleton CP, Byrd BF 3rd, Dokainish H, Edvardsen T, Flachskampf FA, Gillebert TC, Klein AL, Lancellotti P, et al. Recommendations for the evaluation of left ventricular diastolic function by echocardiography: an update from the American Society of Echocardiography and the European Association of Cardiovascular Imaging. *Eur Heart J Cardiovasc Imaging*. 2016;17:1321–1360. doi: 10.1093/ehjci/jew082
38. Galie N, Humbert M, Vachiery JL, Gibbs S, Lang I, Torbicki A, Simonneau G, Peacock A, Vonk Noordegraaf A, Beghetti M, et al; ESC Scientific Document Group. 2015 ESC/ERS guidelines for the diagnosis and treatment of pulmonary hypertension: the Joint Task Force for the Diagnosis and Treatment of Pulmonary Hypertension of the European Society of Cardiology (ESC) and the European Respiratory Society (ERS). *Eur Heart J*. 2016;37:67–119. doi: 10.1093/eurheartj/ehv317
39. Guazzi M, Dixon D, Labate V, Beussink-Nelson L, Bandera F, Cuttica MJ, Shah SJ. RV contractile function and its coupling to pulmonary circulation in heart failure with preserved ejection fraction: stratification of clinical phenotypes and outcomes. *JACC Cardiovasc Imaging*. 2017;10:1211–1221. doi: 10.1016/j.jcmg.2016.12.024
40. Liu D, Hu K, Niemann M, Herrmann S, Cikes M, Stork S, Gaudron PD, Knop S, Ertl G, Bijmens B, et al. Effect of combined systolic and diastolic functional parameter assessment for differentiation of cardiac amyloidosis from other causes of concentric left ventricular hypertrophy. *Circ Cardiovasc Imaging*. 2013;6:1066–1072. doi: 10.1161/CIRCIMAGING.113.000683
41. Phelan D, Collier P, Thavendiranathan P, Popovic ZB, Hanna M, Plana JC, Marwick TH, Thomas JD. Relative apical sparing of longitudinal strain using two-dimensional speckle-tracking echocardiography is both sensitive and specific for the diagnosis of cardiac amyloidosis. *Heart*. 2012;98:1442–1448. doi: 10.1136/heartjnl-2012-302353